Performance Evaluation of Codebook Designs for FD-MIMO with Multiple Panel Array Systems

Hun Min Shin†, Taeseok Oh†, Hanjin Kim†, Jaein Kim†
Haibao Ren*, Yuanjie Li*, Inkyu Lee†, *Fellow, IEEE*
†School of Electrical Eng., Korea University, Seoul, Korea
*Huawei Technologies, Beijing, China
Email: †{semo0617, jets00, hanjin8612, kji_07, inkyu}@korea.ac.kr
*{renhaibao, liyuanjie}@huawei.com

***Abstract*—In this paper, we study full-dimension multiple-input multiple-output (FD-MIMO) systems where a base station is equipped with multiple panel array (MPA) antennas. As the MPA is regarded as a promising means of practical implementation for the FD-MIMO, it is important to characterize a channel modeling and a codebook design. Thus, we first examine the exponential correlation model and the three-dimensional correlation model for the FD-MIMO with MPA. In addition, since antenna elements are not uniformly spaced in the MPA systems, a discrete Fourier transform (DFT) codebook may not be suitable due to phase ambiguity (PA). Thus, we investigation three new codebook design methods which reflect the PA. In numerical results, we confirm that PA compensation and per-panel quantization are effective for MPA systems.**

***Index Terms*—FD-MIMO, Multiple panel array systems, Codebook designs**

I. Introduction

Massive multiple-input multiple-output (MIMO) systems which adopt a large number of antenna elements at a base station (BS) have attracted a great amount of attentions due to its potential of improving spectral efficiency, energy efficiency, and so on [1]. Recently, many researches have investigated the massive MIMO system with various configurations in theoretical aspects [2]–[6]. However, due to some practical implementation issues, the formal standardization of massive MIMO is currently underway.

One of the most concerns in practical massive MIMO systems is how to deploy a large number of antenna elements in the BS's form factor with a limited space. Recently, a full-dimension MIMO (FD-MIMO) communication systems where the antenna elements are placed in a uniform planar array (UPA) has been introduced as a key technology to resolve the spatial limitation at the BS [7]. Due to the two-dimensional (2D) antenna array structure, FD-MIMO systems should consider the signal propagation in both the azimuth and elevation domain [8], whereas the conventional MIMO systems only take the azimuth domain into account. To this end, wireless communication standardization groups such as 3GPP provide the 3D channel model which reflects the geometric structure of the UPA and the propagation effect of the three-dimensional (3D) positions between the BS and user.

A well known problem in FD-MIMO systems is the fact that the number of antenna elements which can be placed in a single panel is limited because of hardware implementation issues. In other words, it is hard to deploy all antenna elements in a single UPA in FD-MIMO systems [9]. One promising solution to this issue is to divide the single large panel into multiple panel array (MPA) using the antenna in package (AIP) techniques [10] which reduces the cost in MPA implementation. On the contrary to the single UPA systems, the antenna elements in MPA systems are not uniformly distributed since each panel is physically separated. Furthermore, even when the panels are not much apart from each other, the radio frequency (RF) chains of panels cannot be perfectly calibrated with respect to the sampling clock timing or the carrier frequency, which results in each panel has different phase offset at each panel [11]. We refer to this phase offset between different panel as phase ambiguity (PA).

Another challenging problem in FD-MIMO systems is its insufficient feedback resources. In the frequency division duplexing (FDD) FD-MIMO systems, it is quite hard to obtain accurate channel state information (CSI) due to large antenna arrays and limited feedback bits. To overcome this issue, a few research efforts have been devoted to design efficient codebook schemes for FD-MIMO configurations [12]–[14]. The authors in [12] demonstrated that the 3D correlation matrix can be well approximated by a Kronecker product of the azimuth and elevation correlation, and designed a product codebook for UPA configurations. Further, an efficient codebook was proposed in [13] which accurately quantizes multiple dominant beam patterns in UPA systems by modifying the Kronecker product discrete Fourier transform (DFT) codebook. Also, in [14], both the symmetric and asymmetric codewords clustering methods for the Kronecker product DFT codebook were suggested. However, since these approaches were only dedicated to the single-panel systems, they may not perform well when it comes to the MPA systems with non-uniformity and PA [15],

This work was supported in part by Huawei Technologies, and in part by National Research Foundation (NRF) funded by the Ministry of Science, ICT & Future Planning (MSIP) of Korea Government under Grant 2017R1A2B3012316.

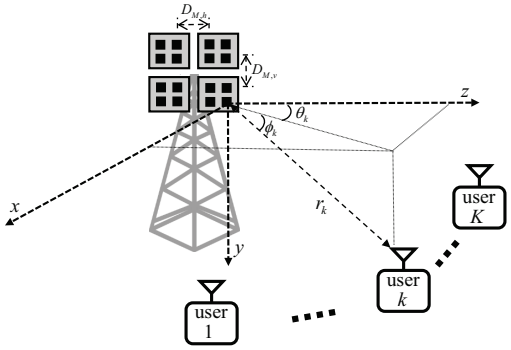

Fig. 1. Illustration of the MPA system

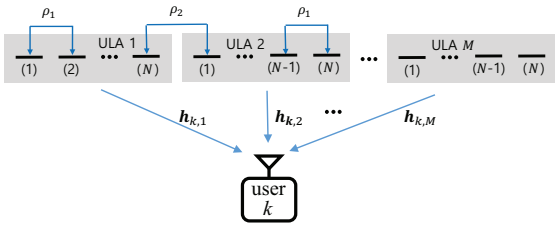

Fig. 2. Exponential model for the multiple uniform linear array panel

and thus we need to consider new codebook designs for MPA systems.

In this paper, we investigate the codebook designs for MPA systems. We first introduce two channel models by extending the exponential correlation model [12] and the 3D correlation model [16] to the MPA systems. To address the aforementioned PA problem, we study three codebook designs which compensate the PA, and then evaluate the performance of the codebook designs by numerical simulations. The numerical results indicate that the PA compensation is a critical factor for codebook designs and it is effective to quantize channel direction information (CDI) of each panel instead of the whole panel.

This paper is organized as follows: Section II introduces two channel models for MPA systems. In Section III, we investigate three codebook designs for the MPA systems. Section IV presents the system performance for various codebook designs through numerical simulations. Finally, the paper is terminated with conclusions in Section V.

Throughout this paper, the boldface capital letters represent matrices and the boldface small letters denote column vectors. In addition, $\mathbf{a}^{\mathrm{T}}$, $\mathbf{a}^{\mathrm{H}}$ and $\mathbf{a}^{*}$ stand for transpose, complex conjugate transpose and conjugate of a vector $\mathbf{a}$, respectively. We designate $\mathbf{A}\otimes\mathbf{B}$ and $[\mathbf{A}]_{i,j}$ as a Kronecker product between two matrices $\mathbf{A}$ and $\mathbf{B}$ and the (i,j)-th element of a matrix $\mathbf{A}$, respectively. Also, $\lceil x \rceil$ denotes the ceiling operation on x

II. System Model

As shown in Fig. 1, we consider multiple UPA systems where a BS is equipped with 2D panel arrays consisting of M_v vertical panels spaced by $D_{M,v}$ and M_h horizontal panels spaced by $D_{M,h}$. It is assumed that each panel array contains N_v and N_h antennas in vertical and horizontal direction, respectively. Also, K users equipped with a single-antenna are served by the BS in the same time and frequency resource. In the following subsections, we examine two different channel models adopted for performance evaluation.

A. Exponential Correlation Model

Since correlation between antennas may significantly affect the overall performance, the spatial correlation must be included in channel modeling. Among various correlation models, we adopt the exponential correlation model which express spatial correlation in terms of the correlation coefficient of neighboring antennas and panel arrays [17]. The exponential correlation model for the multiple UPA has not been characterized in the literature yet, and thus we first extend a single uniform linear array (ULA) to the multiple ULA as in Fig 2. Subsequently, the exponential correlation model for the multiple UPA is established by a Kronecker product of two multiple ULA [12].

Denoting the number of antennas and panel arrays for the multiple ULA as N and M, respectively, the elements of the spatial correlation matrix $\mathbf{R}_{\mathrm{ULA}} \in \mathcal{C}^{MN\times MN}$ for the multiple ULA are given by

$$[\mathbf{R}_{\mathrm{ULA}}]_{i,j} = \rho_1^{|i-j|-\left|\lceil \frac{i}{N} \rceil - \lceil \frac{j}{N} \rceil\right|} \rho_2^{\left|\lceil \frac{i}{N} \rceil - \lceil \frac{j}{N} \rceil\right|}, \quad (1)$$

where ρ_1 and ρ_2 indicate the correlation coefficient of neighboring antennas and panel arrays, respectively. Then, the correlated channel of user k can be expressed by stacking the channel vectors as

$$\mathbf{h}_k^H = [\mathbf{h}_{k,1}^H \cdots \mathbf{h}_{k,M}{}^H] = \tilde{\mathbf{h}}_k^H \mathbf{R}_{\mathrm{ULA}}^{\frac{1}{2}} \quad \in \mathcal{C}^{1\times MN}, \quad (2)$$

where $\mathbf{h}_{k,m}^H \sim \mathcal{CN}(\mathbf{0}, \mathbf{I}_{MN}) \in \mathcal{C}^{1\times N}$ is the channel vector from the m-th panel array and $\tilde{\mathbf{h}}_k^H \in \mathcal{C}^{1\times MN}$ represents a complex Gaussian random vector with zero mean and covariance matrix $\mathbf{I}_{MN}$.

Based on the result of [12], the spatial correlation matrix of the multiple UPA can be obtained as

$$\mathbf{R}_{\mathrm{UPA}} = \mathbf{R}_v \otimes \mathbf{R}_h, \quad (3)$$

where $\mathbf{R}_v$ and $\mathbf{R}_h$ equal the spatial correlation matrix of the vertical and horizontal ULA, respectively. Finally, the correlated channel vector of user k for the multiple UPA can be written as

$$\mathbf{h}_k^H = \mathbf{vec}(\mathbf{H}_k) = \bar{\mathbf{h}}_k \mathbf{R}_{\mathrm{UPA}}{}^{\frac{1}{2}} \quad \in \mathcal{C}^{1\times M_v N_v N_h N_h}, \quad (4)$$

where the aggregate channel matrix $\mathbf{H}_k \in \mathcal{C}^{M_v N_v \times M_h N_h}$ is defined as

$$\mathbf{H}_k = \begin{bmatrix} \tilde{\mathbf{H}}_{k,1,1} & \cdots & \tilde{\mathbf{H}}_{k,1,M_h} \\ \vdots & \ddots & \vdots \\ \tilde{\mathbf{H}}_{k,M_v,1} & \cdots & \tilde{\mathbf{H}}_{k,M_v,M_h} \end{bmatrix}, \quad (5)$$

and $\bar{\mathbf{h}}_k \sim \mathcal{CN}(\mathbf{0}, \mathbf{I}_{M_v N_v N_v N_h}) \in \mathcal{C}^{1\times M_v N_v N_v N_h}$ stands for the complex Gaussian channel vector. Here, $\tilde{\mathbf{H}}_{k,m_v,m_h}$ indicates the channel matrix from the m_v-th row and the m_h-th column pannel.

B. 3D Correlation Model

Unlike the exponential correlation model, where the effect of $D_{M,v}$ and $D_{M,h}$ is implicit in the modeling, the 3D correlation model can explicitly show the impact of panel spacing. Thus, we extend the 3D correlation model introduced in [16] to the multiple UPA with different antenna spacing in horizontal and vertical directions. Assuming a multi-path channel, the aggregate channel matrix between the BS and the k-th user $\mathbf{H}_k \in \mathcal{C}^{M_v N_v \times M_h N_h}$ is given by

$$\mathbf{H}_k = \frac{1}{\sqrt{P}} \sum_{p=1}^{P} \mathbf{H}_k^p, \tag{6}$$

where P represents the number of paths, and $\mathbf{H}_k^p$ is the aggregate channel matrix of the p-th path.

Denoting $\rho_k^p(r_k) = z^p \sqrt{-\gamma(r_k)/10}$ as the large-scale fading coefficient where z^p is the random complex coefficient with zero mean and unit variance and $\gamma(r_k) = 34.5{+}10\alpha \log r_k$ with the pathloss exponent α, the $(n_v, n_h)^{th}$ element is expressed as

$$[\mathbf{H}_k^p]_{n_v,n_h} = \rho_k^p\left(r_k\right) \exp\left\{\tfrac{2\pi}{\lambda}\left(\Delta_{v,n_v} \sin\beta_k^p + \Delta_{h,n_h} \cos\theta_k^p \cos\beta_k^p\right)\right\} \tag{7}$$

in which $\Delta_{v,n_v} = D_{M,v}\left(\left\lceil \frac{n_v}{N_v} \right\rceil - 1\right) + D_{N,v}\left(n_v - \left\lceil \frac{n_v}{N_v} \right\rceil\right)$ and $\Delta_{h,n_h} = D_{M,h}\left(\left\lceil \frac{n_h}{N_h} \right\rceil - 1\right) + D_{N,h}\left(n_h - \left\lceil \frac{n_h}{N_h} \right\rceil\right)$. Also, β_k^p and θ_k^p indicate the angle of arrival of user k at the p-th path in the vertical and horizontal domain, respectively, λ is the wavelength. By inspecting equation (7), we can see that the phase of the channel element varies by the panel arrays, while the magnitude is fixed regardless of panel arrays. Then, the channel vector of user k for the multiple UPA becomes $\mathbf{vec}(\mathbf{H}_k)$.

In the following section, we investigate the codebook designs for MPA systems. For reference, one can employ the $M_v N_v M_h N_h \times 2^B$ conventional DFT codebook $\mathcal{C}_{\text{conv}}$ [12] which is defined as a Kronecker product between two codebooks $\mathcal{C}_{\text{conv},v} \in \mathbb{C}^{M_v N_v \times 2^{B_v}}$ and $\mathcal{C}_{\text{conv},h} \in \mathbb{C}^{M_h N_h \times 2^{B_h}}$. Here, $\mathcal{C}_{\text{conv},v}$ and $\mathcal{C}_{\text{conv},h}$ correspond to the DFT codebook for the vertical and horizontal domain, respectively, and can be expressed as

$$\begin{aligned}
[\mathcal{C}_{\text{conv},v}]_{n_v,b_v} &= \frac{1}{\sqrt{M_v N_v}} \exp\left(\frac{-j2\pi(n_v-1)(b_v-1)}{2^{B_v}}\right), \\
[\mathcal{C}_{\text{conv},h}]_{n_h,b_h} &= \frac{1}{\sqrt{M_h N_h}} \exp\left(\frac{-j2\pi(n_h-1)(b_h-1)}{2^{B_h}}\right),
\end{aligned} \tag{8}$$

where B_v and B_h are the feedback bits allocated to the vertical and horizontal domain, respectively. Then, the aggregate channel vector for user k can be quantized as

$$\hat{\mathbf{h}}_k = \arg\max_{\mathbf{c}\in\mathcal{C}_{\text{conv}}} \left|\mathbf{h}_k^{\text{H}} \mathbf{c}\right|.$$

However, since the conventional DFT codebook has been designed for the single-panel systems with the regular spatial correlation owing to evenly spaced antenna elements, it was reported that the DFT codebook incurs some performance degradation in MPA systems [15]. This is due to the fact that physically separated panels in MPA systems cause irregular spatial correlation and the corresponding phase difference [18].

III. Codebook Designs for MPA systems

In this section, we present three different codebook designs for MPA systems. First, we can simply modify the conventional DFT codebook based on the 3D correlation model (6). From the PAs between different panels in (7), we can define the panel spacing compensation factor for the vertical and horizontal domain δ_{v,n_v} and δ_{h,n_h} with distance $D_{M,v}$ and $D_{M,h}$ as

$$\begin{aligned}
\delta_{v,n_v} &= \left(\left\lceil \frac{n_v}{N_v} \right\rceil - 1\right)\left(\frac{D_{M,v}}{D_{N,v}} - 1\right), \\
\delta_{h,n_h} &= \left(\left\lceil \frac{n_h}{N_h} \right\rceil - 1\right)\left(\frac{D_{M,h}}{D_{N,h}} - 1\right),
\end{aligned}$$

respectively.

Then, we provide the panel spacing aware codebook (PSC) $\mathcal{C}_{\text{PSC}} = \mathcal{C}_{\text{PSC},v} \otimes \mathcal{C}_{\text{PSC},h}$ where

$$\begin{aligned}
[\mathcal{C}_{\text{PSC},v}]_{n_v,b_v} &= \frac{1}{\sqrt{M_v N_v}} \exp\left(\frac{-j2\pi\left(n_v{-}1{+}\delta_{v,n_v}\right)(b_v{-}1)}{2^{B_v}}\right), \\
[\mathcal{C}_{\text{PSC},h}]_{n_h,b_h} &= \frac{1}{\sqrt{M_h N_h}} \exp\left(\frac{-j2\pi(n_h{-}1{+}\delta_{h,n_h})(b_h{-}1)}{2^{B_h}}\right).
\end{aligned} \tag{9}$$

By adding the panel spacing compensation factors δ_{v,n_v} and δ_{h,n_h}, it is expected that the modified codebook (9) captures irregular correlation in the MPA configurations better than the conventional codebook (8). Note that the conventional DFT codebook and the PSC directly quantize the aggregated channel vector $\mathbf{h}_k$ of length $M_v N_v M_h N_h$, and thus the quantization for individual panel may be inaccurate with finite feedback bits so that a performance degradation can be incurred. To tackle this issue, we may consider a per-panel codebook (PPC) which quantizes CDI in a panel-wise manner.

Here, we introduce two different codebook design methods based on PPC in the following. The first scheme, which is called type-I multi-panel (MP) codebook [19], quantizes the channel vector $\mathbf{h}_k$ and is defined as

$$\mathcal{C}_{\text{type-I}} = \mathbf{\Theta} \otimes \mathcal{C}_{\text{PPC}},$$

where $\mathbf{\Theta}$ indicates a $M_v M_h \times 4^{M_v M_h - 1}$ matrix whose columns are determined by $[1, e^{j\theta_2}, \cdots, e^{j\theta_{M_v M_h}}]$ with $\theta \in \{0, \frac{\pi}{2}, \pi, \frac{3\pi}{2}\}$, and $\mathcal{C}_{\text{PPC}} \in \mathbb{C}^{N_v N_h \times 2^{B_{\text{CDI}}}}$ denotes a conventional DFT codebook for a single panel. Since each PA is

quantized by 2 bits in this scheme, the total number of feedback bits B can be expressed as $B = B_{\text{CDI}} + 2(M_v M_h - 1)$, where B_{CDI} is the number of feedback bits for CDI.

In the second PPC-based codebook design method, which is called independent-panel codebook (IPC), each user k separately quantizes $\mathbf{h}_{k,m}$ for $m = 1, \ldots, M_v M_h$ from $\mathcal{C}_{\text{PPC}}$ as

$$\hat{\mathbf{h}}_{m,k} = \arg\max_{\mathbf{c} \in \mathcal{C}_{\text{PPC}}} \left| \mathbf{h}_{m,k}^{\text{H}} \mathbf{c} \right|.$$

Further, to compensate the PAs, the k-th user also quantizes $M_v M_h - 1$ PAs with a uniformly quantized PA codebook of length $2^{B_{\text{p}}}$, i.e., $\left\{0, \frac{2\pi}{2^{B_{\text{p}}}}, \cdots, \frac{2(2^{B_{\text{p}}-1})\pi}{2^{B_{\text{p}}}}\right\}$, and then reconstructs the aggregate channel $\hat{\mathbf{h}}_k$ as

$$\hat{\mathbf{h}}_k^{\text{H}} = \left[\hat{\mathbf{h}}_{1,k}^{\text{H}}, \cdots, \hat{\mathbf{h}}_{m,k}^{\text{H}} e^{j\hat{\theta}_m}, \cdots, \hat{\mathbf{h}}_{M_v M_h, k}^{\text{H}} e^{j\hat{\theta}_{M_v M_h - 1}}\right], \quad (10)$$

where the total number of feedback bits B becomes $B = M_v M_h B_{\text{CDI}} + (M_v M_h - 1) B_{\text{p}}$.

Finally, we provide the search complexity of channel quantization for all codebook designs. The search complexity of the conventional codebook, PSC, and type-I MP codebook equals their codebook size of 2^B. On the other hand, the per-panel codebook size and PA codebook size of the IPC scheme are $2^{B_{\text{CDI}}}$ and $2^{B_{\text{p}}}$, respectively, and the consequent search complexity of the IPC scheme is given by $M_v M_h 2^{B_{\text{CDI}}} + (M_v M_h - 1) 2^{B_{\text{p}}}$, which is much smaller compare to other schemes for the same number of total feedback bits.

IV. Simulation Results

In this section, we compare the average sum-rate performance of the conventional DFT codebook, the PSC, the IPC and type-I MP codebook for both the exponential correlation and the 3D correlation models with zero-forcing (ZF) beamforming and maximum ratio transmission (MRT). For the IPC scheme, we find the optimal B_{p} by exhaustively search. The detailed simulation configurations are described in Table I.

In Fig. 3, the average sum-rate performance of various schemes are exhibited in terms of the inter-panel correlation coefficient ρ_2 for the exponential channel model with $B = 22$, $M_v = 2$, $M_h = 2$, $N_h = 2$, and $N_v = 2$. First, it can be observed for every codebook designs that the average sum-rate performance keeps decreasing as the inter-panel correlation ρ_2 increases. Especially, a performance loss of IPC is shown to be 23 % at $\rho_2 = 0.9$ compared to the case of $\rho_2 = 0$, which implies that a multi-user gain highly depends on inter-panel correlation. Next, we can check that IPC and type-I MP codebook outperform the conventional codebook, because the conventional codebook neglects discontinuity between different panels. Thus, we conclude that the PA compensation between different panels is essential to improve the average sum-rate performance. In addition, it is noticeable that IPC shows remarkable a performance gain compared to the other schemes. Therefore, we can see that CDI for MPA systems should be individually quantized with respect to each panel.

Fig. 4 illustrates the average sumrate performance with respect to the normalized panel spacing d_p which is normalized

TABLE I
Simulation Setup

Number of users K	3
Distance between a BS and a user d_k	150 m
Carrier frequency f	6 GHz
Path-loss exponent α	3.5
Complex small-scale fading gain variance σ_z^2	1
Distance of neighboring antennas in elevation domain $D_{N,v}$	0.5λ
Distance of neighboring antennas in azimuth domain $D_{N,h}$	0.5λ
Height of a BS	35 m
Height of a user	1.5 m
Angle-of arrival in azimuth domain θ_k^p	$U[0, \pi]$
Angle-of arrival in elevation domain β_k^p	$U[0, \pi/36]$
Number of paths P	20
Transmit power at a BS	24 dBm
Bandwidth	10 MHz
Noise figure	7 dB
Correlation coefficient of neighboring antennas ρ_1	0.9

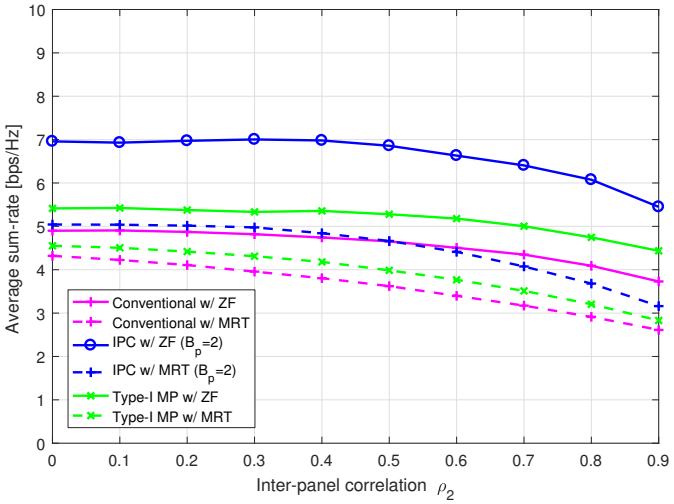

Fig. 3. Average sum-rate performance for the exponential correlation model with $B = 22$, $M_h = 2$, $M_v = 2$, $N_h = 2$ and $N_v = 2$

with the wavelength λ for the 3D correlation model with $B = 22$, $M_v = 2$, $M_h = 2$, $N_h = 2$ and $N_v = 2$. Similar to Fig. 3, the IPC performs the best among all schemes. We can check that the average sum-rate of all schemes becomes larger as d_p grows. This is because the correlation between different panels tends to decrease as the panel spacing increases, which accords with the results in Fig. 3. Also, it is observed that the average sum-rate performance of IPC and PSC increase more rapidly with d_p as compared to that of the conventional codebook and the type-I MP codebook, since IPC and PSC effectively render the effect of the panel spacing.

Fig. 5 depicts the average sum-rate performance with respect to the total number of feedback bits B for the 3D correlation channel model with $M_v = 2$, $M_h = 1$, $N_h = 4$ and $N_v = 4$. As seen in this figure, the performance of the conventional DFT codebook, PSC and type 1 MP codebook

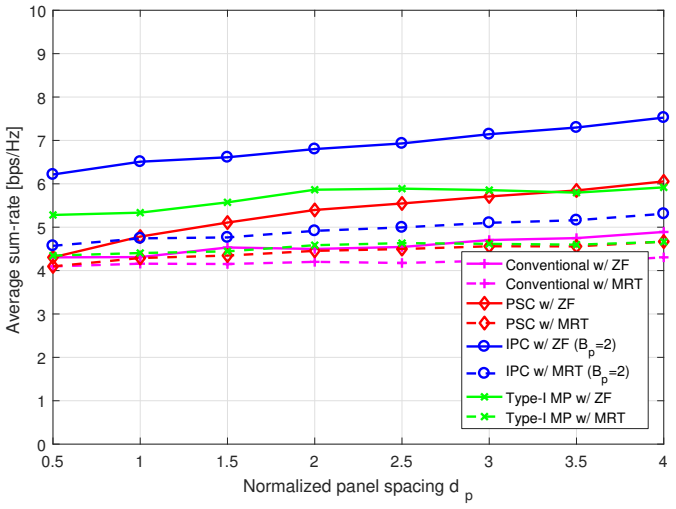

Fig. 4. Average sum-rate performance for the 3D correlation model with $B = 22$, $M_h = 2$, $M_v = 2$, $N_h = 2$ and $N_v = 2$

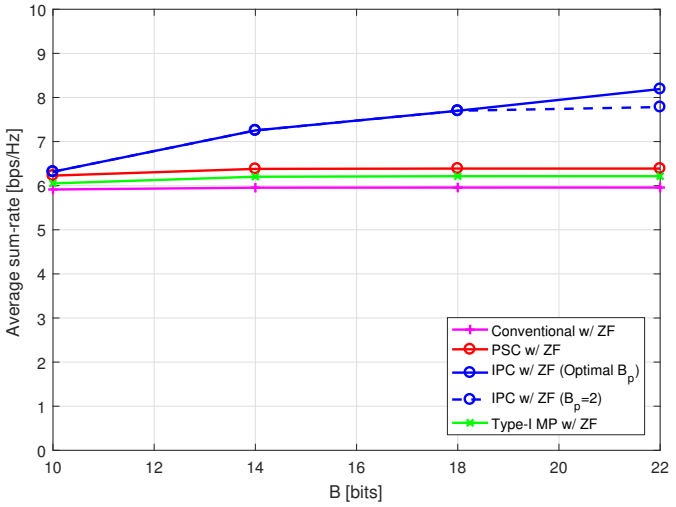

Fig. 5. Average sum-rate performance for the 3D correlation model with $M_h = 1$, $M_v = 2$, $N_h = 4$ and $N_v = 4$

become saturated as B increases, while that of IPC grows consistently. Thus, it is more beneficial to employ the IPC scheme than a joint panel codebook for the same number of feedback bits. Also, it can be shown that the performance of IPC with $B_p = 2$ is the same as that of IPC with optimal B_p for B less than 18. Throughout the simulations, we confirm that PA compensation and per-panel CDI quantization are efficient for MPA systems.

V. Conclusion

In this paper, we have studied the performance of codebook designs for MPA systems. To evaluate the performance, we first have introduced two channel models by extending the exponential correlation model and the 3D correlation model to MPA systems. Then, we have investigated three codebook designs. PSC, type-I MP codebook and IPC which take into account PA and compensate the PA in different fashions, and we have compared the performance of codebook designs for MPA systems by numerical simulations. In numerical results, we have confirmed that PA compensation and panel-wise CDI quantization are required for MPA systems to achieve better performance compared to the conventional scheme.

References

[1] E. G. Larsson, O. Edfors, F. Tufvesson, and T. L. Marzetta, "Massive MIMO for Next Generation Wireless Systems," *IEEE Commun. Mag.*, vol. 52, pp. 186–195, Feb. 2014.

[2] T. L. Marzetta, "Noncooperative Cellular Wireless with Unlimited Numbers of Base Station Antennas," *IEEE Trans. Wireless Commun.*, vol. 9, pp. 3590–3600, Nov. 2010.

[3] Y. Jeon, C. Song, S.-R. Lee, S. Maeng, J. Jung, and I. Lee, "New Beamforming Designs for Joint Spatial Division and Multiplexing in Large-Scale Multi-user MISO Systems," *IEEE Trans. on Wireless Commun.*, vol. 16, pp. 3029–3041, May 2017.

[4] S.-R. Lee, J. Jung, H. Park, and I. Lee, "A New Energy Efficient Beamforming Strategy for MISO Interfering Broadcast Channels based on Large Systems Analysis," *IEEE Trans. on Wireless Commun.*, vol. 15, pp. 2872–2882, Apr. 2016.

[5] S.-R. Lee, H.-B. Kong, H. Park, and I. Lee, "A New Beamforming Design Based on Random Matrix Theory for Weighted Sum-Rate Maximization in Interference Channels," *in Proc. IEEE Global Communications Conference*, pp. 3719–3724, Dec. 2016.

[6] J. Kim, S.-H. Park, O. Simeone, I. Lee, and S. S. Shitz, "Joint Design of Digital and Analog Processing for Downlink C-RAN with Large-Scale Antenna Arrays," *in Proc. IEEE Signal Processing Advances in Wireless Communications*, Jul. 2017.

[7] H. Ji, Y. Kim, J. Lee, E. Onggosanusi, Y. Nam, J. Zhang, B. Lee, and B. Shim, "Overview of Full-Dimension MIMO in LTE-Advanced Pro," *IEEE Communications Magazine*, vol. 55, pp. 176–184, Feb. 2017.

[8] W. Lee, S.-R. Lee, H.-B. Kong, S. Lee, and I. Lee, "Downlink vertical beamforming designs for active antenna systems," *IEEE Transactions on Communications*, vol. 62, no. 6, pp. 1897–1907, 2014.

[9] Ericsson, "Type I Multi-panel CSI codebook," Tech. Rep. R1-1702684, 3GPP TSG-RAN WG1, Feb. 2017.

[10] Y. P. Zhang and D. Liu, "Antenna-on-chip and antenna-in-package solutions to highly integrated millimeter-wave devices for wireless communications," *IEEE Transactions on Antennas and Propagation*, vol. 57, pp. 2830–2841, Aug. 2009.

[11] CATT, "Multi-panel/multi-TRP transmission," Tech. Rep. R1-1702071, 3GPP TSG-RAN WG1, Feb. 2017.

[12] D. Ying, F. W. Vook, T. A. Thomas, D. J. Love, and A. Ghosh, "Kronecker product correlation model and limited feedback codebook design in a 3D channel model," *in Proc. IEEE International Conference on Commun.*,, pp. 5865–5870, Jun. 2014.

[13] J. Choi, K. Lee, D. J. Love, T. Kim, and R. W. Heath, "Advanced Limited Feedback Designs for FD-MIMO Using Uniform Planar Arrays," *in Proc. IEEE Global Communications Conference*, Dec. 2015.

[14] Y. Xie, S. Jin, J. Wang, Y. Zhu, X. Gao, and Y. Huang, "A Limited Feedback Scheme for 3D Multiuser MIMO based on Kronecker Product Codebook," *in Proc. IEEE International Symposium on Personal, Indoor and Mobile Radio Communications (PIMRC)*, pp. 1130–1135, Sep. 2013.

[15] Huawei and Hisilicon, "DL Codebook Design for Multi-panel Structured MIMO in NR," Tech. Rep. R1-1700066, 3GPP TSG-RAN WG1, Jan. 2017.

[16] W. Liu, Z. Wang, C. Sun, S. Chen, and L. Hanzo, "Structured non-uniformly spaced rectangular antenna array design for FD-MIMO systems," *IEEE Trans. on Wireless Commun.*, vol. 16, no. 5, pp. 3252–3266, 2017.

[17] S. L. Loyka, "Channel capacity of mimo architecture using the exponential correlation matrix," *IEEE Commun. Lett.*, vol. 5, no. 9, pp. 369–371, 2001.

[18] F. Yuan and C. Yang, "Bit Allocation Between Per-cell Codebook and Phase Ambiguity Quantization for Limited Feedback Coordinated Multi-point Transmission Systems," *IEEE Transactions on Communications*, vol. 60, pp. 2546–2559, Jul. 2012.

[19] Huawei et al., "WF on Type I and II CSI Codebooks," Tech. Rep. R1-1709232, 3GPP TSG-RAN WG1, May. 2017.